Biophysical Chemistry 155 (2011) 82–88

Contents lists available at ScienceDirect

Biophysical Chemistry

journal homepage: http://www.elsevier.com/locate/biophyschem

HIV-integrase aptamer folds into a parallel quadruplex: A thermodynamic study

Sean Kelley [a], Salome Boroda [a], Karin Musier-Forsyth [a,b,c], Besik I. Kankia [a,c,*]

[a] Department of Chemistry, The Ohio State University, Columbus OH 43210, USA
[b] Department of Biochemistry, The Ohio State University, Columbus OH 43210, USA
[c] Center for RNA Biology, The Ohio State University, Columbus OH 43210, USA

ARTICLE INFO

Article history:
Received 20 January 2011
Received in revised form 3 March 2011
Accepted 3 March 2011
Available online 9 March 2011

Keywords:
DNA quadruplexes
G-quartets
HIV-integrase aptamer
Thermodynamics
Calorimetry
Circular dichroism

ABSTRACT

Short guanine-rich sequences have a tendency to form quadruplexes that are stabilized by G-quartets with specific cation coordination. Quadruplexes are part of telomeres at the ends of chromosomes and play an important role in the regulation of gene expression. In addition, there is a strong interest in the therapeutic and biotechnological potential of quadruplex oligonucleotides. The HIV-integrase aptamer, $d(GGGT)_4$, demonstrated unusually favorable van't Hoff thermodynamics, and based on NMR studies the aptamer was proposed to fold into an antiparallel structure. Here we probed an apparent discrepancy between the NMR structure and the quadruplex topology suggested by circular dichroism (CD). Systematic thermodynamic analyses of $d(GGGT)_4$ and variants containing sequence modifications or missing specific nucleotides are consistent with a parallel quadruplex fold. CD studies carried out over a wide concentration range did not support a possible structural transition upon increasing strand concentration. Taken together, both optical and thermodynamic studies performed here strongly support a parallel fold for the $d(GGGT)_4$ aptamer.

1. Introduction

Short guanine-rich sequences fold into a structure known as a G-quartet or quadruplex, which is formed by four guanine residues associated in a square planar configuration. Each base interacts with its two neighbors through Hoogsteen hydrogen bonds (8 per quartet). The formation of stable quadruplexes requires certain metal ions (e.g., K^+ or Sr^{2+}) that bind specifically to guanine O6 carbonyl groups in the inner core of G-quartets. Owing to the cation coordination, hydrogen bonds and stacking interactions between G-quartets, quadruplexes are very stable.

It is believed that quadruplexes are involved in the regulation of gene expression and are part of telomeres at the ends of chromosomes [1–6]. Quadruplexes are also found commonly in DNA aptamers, which are very useful in biotechnological and therapeutic applications as they offer specific molecular recognition properties [7–11]. Earlier studies have shown that quadruplexes possess intrinsic optical properties (i.e., absorb light at 300 nm) that distinguish them from other secondary structures [12–14]. We have developed quadruplex-formation assays, which exploits this unique optical property to study enzymes that cleave DNA [15] or facilitate strand-exchange reactions [12]. The free energy of DNA quadruplexes can also be used to drive unfavorable (endergonic) reactions of nucleic acids (e.g., isothermal PCR) [16].

The key feature of quadruplex-driven reactions is that some DNA sequences are capable of forming quadruplexes with significantly more favorable thermodynamics than the corresponding DNA duplexes. The quadruplex-forming sequence $d(GGGT)_4$, which is a potent HIV-1 integrase inhibitor [17], was previously shown to display extraordinary stability and unusually favorable van't Hoff thermodynamics [10]. The folding topology of $d(GGGT)_4$ was previously investigated by CD spectroscopy, which suggested formation of a parallel quadruplex in solution, with all four guanine tracks oriented in the same direction [17–19]. In contrast, a solution NMR spectroscopy study concluded that the same sequence formed an antiparallel quadruplex [9]. Due to the therapeutic potential of HIV-1 integrase aptamer [17], as well as its utility in biotechnological applications [16], a detailed thermodynamic analysis of $d(GGGT)_4$ was performed in order to resolve the apparent discrepancy between the NMR-derived structure and the quadruplex topology suggested CD. Based on CD, UV melting and calorimetric studies of wild-type and variant $d(GGGT)_4$ sequence, we conclude that $d(GGGT)_4$ folds into a parallel quadruplex.

2. Materials and methods

2.1. Materials

DNA oligonucleotides were obtained from Integrated DNA Technologies and their concentration was determined by measuring UV absorption at 260 nm, as described earlier [20]. All measurements were performed in a buffer consisting of 10 mM Tris–HCl, pH 8.7 and ionic strength was adjusted by addition of appropriate salt, KCl and/or CsCl. DNA samples were annealed by incubation at 80 °C for a few min and slow cooling to room temperature.

* Corresponding author at: Department of Chemistry, The Ohio State University, Columbus OH 43210, USA. Tel.: +1 614 688 8799; fax: +1 614 688 5402.
E-mail address: bkankia@chemistry.ohio-state.edu (B.I. Kankia).

0301-4622/$ – see front matter © 2011 Elsevier B.V. All rights reserved.
doi:10.1016/j.bpc.2011.03.004

2.2. CD spectroscopy

CD spectra were obtained with a JASCO J710 spectropolarimeter equipped with thermoelectrically-controlled cell holders. Quartz cells with 1 cm and 0.05 cm path lengths were used to study the concentration-dependence of the CD profile.

2.3. UV spectroscopy

UV absorbance spectra were recorded on a Varian UV–visible spectrophotometer (Cary-100 Bio) equipped with thermoelectrically-controlled cell holders. Absorbance versus temperature profiles (melting curves) were measured at either 240 nm, 260 nm or 295 nm in 1 cm, 0.5 cm or 0.05 cm path-length cells. Samples were incubated at 80 °C for a few min in the cell holder prior to ramping the temperature to the desired starting temperature. The melting experiments were performed at a heating rate 0.5 °C per min. Melting curves allowed an estimation of melting temperature, T_m, the midpoint temperature of the unfolding process. Van't Hoff enthalpies, ΔH_{vH}, were calculated using the equation $\Delta H_{vH} = 4\,R\,T_m^2\,\delta\alpha/\delta T$ where, R is the gas constant and $\delta\alpha/\delta T$ is the slope of the normalized optical absorbance versus temperature curve at T_m [21].

2.4. ITC measurements

A MicroCal VP-ITC calorimeter was used to measure the heat evolved during quadruplex formation. The oligonucleotide solution was placed in the reaction cell and titrated with K^+ ions. Typically, 5–20 μL aliquots of KCl solution (3 mM) were injected into the oligonucleotide solution (15 μM) via a syringe spinning at 400 rpm. The resulting curves were corrected by subtracting the signal obtained from control experiments in which the cation solutions were injected into the buffer. Reverse titrations also were performed wherein 5 μL aliquots of the oligonucleotide solution (150 uM) were titrated into a 3 mM KCl solution. The latter experiments were designed to measure quadruplex-formation heats, which were determined by integrating and averaging the peaks of the initial injections. This was possible because the solution concentrations used in the experiments were greater than the inverse of the binding constant. The resulting curves of the inverse titrations were corrected using two control experiments: in one case buffer was injected into the KCl solution and in the second control oligonucleotide was injected in buffer solution without KCl. The data analysis program provided by MicroCal was used to obtain the number of binding sites, n, the binding constants, K, and the enthalpy of binding, ΔH.

3. Results and discussion

3.1. CD measurements of $(GGGT)_4$

CD spectroscopy has traditionally been used to gain information about the folding topology of DNA quadruplexes. By comparing CD spectra with NMR or X-ray structures of simple GT-containing sequences, the following features are observed: In the presence of K^+ ions, antiparallel quadruplexes demonstrate positive CD bands with maxima at ~245 nm and ~295 nm and a negative peak at ~265 nm, while parallel quadruplexes show a strong positive peak at ~265 nm and a negative peak of lesser intensity at ~240 nm [22–24]. In addition, characteristics of parallel quadruplexes also include a minor positive peak at ~305 nm [22,25–27]. Quadruplexes containing loops and G-segments with variable lengths or containing complementary loop nucleotides [24,28–30] or chemical modifications ([31] and references therein) demonstrate more complicated CD profiles. For instance, the CD profile of the parallel quadruplex d(TAGGGUTAGGGT) dimer shows an additional maximum at ~290 nm [29,30]. Thus, although CD spectrometry cannot unambiguously determine the topology of all quadruplexes, in the case of simple GT-containing sequences with regular G and T segments, such as $(GGGT)_4$, CD is a useful tool for generating an initial structural model.

Fig. 1A shows the CD spectra of $(GGGT)_4$ (solid line) and of the thrombin binding aptamer (TBA), GGTTGGTGTGGTTGG (dashed line), in the presence of 50 mM KCl. The spectrum of TBA is shown here as an example of an antiparallel conformation with the characteristic peaks described above. Previous structural studies both in solution [32,33] and in crystals [34] confirmed the antiparallel fold. In construct, the CD spectrum of $(GGGT)_4$ reveals a typical parallel fold with positive maxima at 245 nm and 305 nm, and a negative peak at 265 nm. An earlier NMR study concluded that $(GGGT)_4$ possesses an antiparallel fold with two G-quartets and two T-G-T-G loops [9], which is in obvious disagreement with the CD spectra shown in Fig. 1A and published earlier [17–19]. Note that the NMR analysis was carried out using $(GGGT)_4$ with phosphorothioate linkages at the ends. However, it is unlikely that these modifications affect the folding topology since CD analysis of both modified and unmodified sequences revealed identical spectra [17,35]. Since NMR experiments are typically conducted in concentrated solutions, the discrepancy between the NMR and CD data may reflect concentration differences. To investigate this possibility, CD measurements were performed as a function of oligonucleotide concentration. Since accurate CD profiles can only be recorded for samples that measure <1 optical density (OD) unit, 0.05 cm cells were used for these studies. This allowed CD spectra to be measured at 120 μM $(GGGT)_4$. The 20-fold increase in concentration did not reveal any measurable changes in molar elipticity relative to the spectrum shown in Fig. 1A (data not shown).

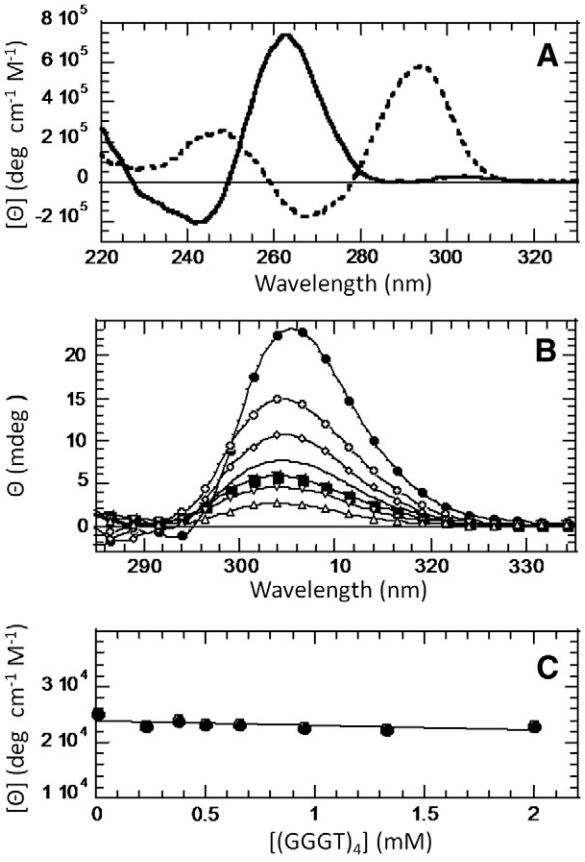

Fig. 1. (A) CD spectra of $(GGGT)_4$ and TBA quadruplexes at 6 uM concentration in the presence of 50 mM KCl at 20 °C measured in a 1-cm cell; (B) Concentration dependence of CD spectra measured in 0.023 mM–2 mM intervals in 0.05-cm cell; (C) Concentration dependence of the molar elipticity of $(GGGT)_4$ at 305 nm.

Although, 120 μM is the highest concentration at which the entire spectrum can be reliably determined in a 0.05 cm cell, one can accurately monitor CD signals of significantly more concentrated solutions in the long-wavelength region of the spectrum. In this region, nucleic acids are almost transparent but antiparallel quadruplexes display a strong positive CD signal [36]. If an increase in $(GGGT)_4$ concentration is accompanied by a change in topology from parallel to antiparallel, then a strong CD signal should appear at 295 nm. Fig. 1B shows the CD spectrum of 2 mM solution of $(GGGT)_4$ (top curve) and the effects of dilution down to 23 μM. The peak at 305 nm in Fig. 1B represents the minor positive signal characteristic of antiparallel structures (see Fig. 1A). The concentration dependence of the molar ellipticity at 305 nm demonstrates a linear dependence from 6 μM to 2 mM strand concentration (Fig. 1C), which clearly indicates that $(GGGT)_4$ maintains its parallel conformation at higher concentrations. Thus, the discrepancy between NMR and CD data cannot be explained by differences in experimental concentrations of $(GGGT)_4$.

3.2. UV melting studies of $(GGGT)_4$

Temperature-dependent UV spectroscopy is a convenient tool to study thermal stability and estimate van't Hoff thermodynamics of DNA secondary structures. Unfolding of DNA duplexes is accompanied by an increase in absorbance at 260 nm, whereas unfolding of nucleic acid triplexes is better characterized at 280 nm [37], and accurate determination of the thermodynamic parameters for quadruplexes is possible by monitoring the long-wavelength region of the UV spectrum (~300 nm) [12,13,36]. To reveal suitable optical windows for monitoring quadruplex unfolding, we recorded UV spectra of $(GGGT)_4$ in the presence and absence of 5 mM K^+ ions, which revealed three peaks at 240 nm, 260 nm, and 295 nm (Fig. 2A). The melting profiles at these wavelengths are shown in Fig. 2B. All three profiles reveal common transitions at 86 °C, which correspond to quadruplex unfolding. While UV measurements at 295 nm are sensitive only to quadruplex unfolding, measurements at 240 nm and 260 nm reveal some perturbation before the main peak. Therefore, all UV melting experiments were performed at 295 nm. The melting profiles reveal monophasic transitions, which are characteristic of a two-state process (Figs. 2B and 5). To confirm that the transition is monophasic, an additional dual wavelength test was performed [38]. In particular, plots of the absorbance at a particular wavelength (i.e., 260 nm) versus the absorbance measured at a second wavelength (i.e., 295 nm) were linear (data not shown). This linear dependence supports the two-state nature of the transition [38].

As shown in Fig. 2B, the $(GGGT)_4$ quadruplex is very stable; in the presence of 5 mM K^+ ions it melts at 86 °C, which is in good agreement with previous studies [10]. Under these conditions, the stability is too high to perform an accurate van't Hoff analysis (Fig. 2B). To determine suitable concentrations for the analysis, we studied the thermal stability of the quadruplex as a function of K^+ concentration (Fig. 3). Increasing the K^+ concentration over the concentration range 0.5–10 mM results in a linear increase of the thermal stability from 75 °C to 90 °C. At $[K^+] < 0.5$ mM, a sudden drop of the T_m is observed, which indicates that at these concentrations the quadruplex is only partially folded or changes its structure.

UV unfolding experiments performed at different strand concentrations allowed an estimation of both the molecularity of the complex and the van't Hoff enthalpy, ΔH_{vH} [21]. Our experiments over a 60-fold concentration range (from 2 μM to 120 μM) revealed that the thermal stability of $(GGGT)_4$ is essentially independent of the strand concentration (data not shown). This agrees well with previous studies [17] and confirms the formation of a mono-molecular structure. Since T_m is independent of the strand concentration, ΔH_{vH} could not be estimated from the concentration dependence. However, a shape analysis of the melting curves as described in Materials and Methods revealed a ΔH_{vH} value of -62 ± 6 kcal/mol.

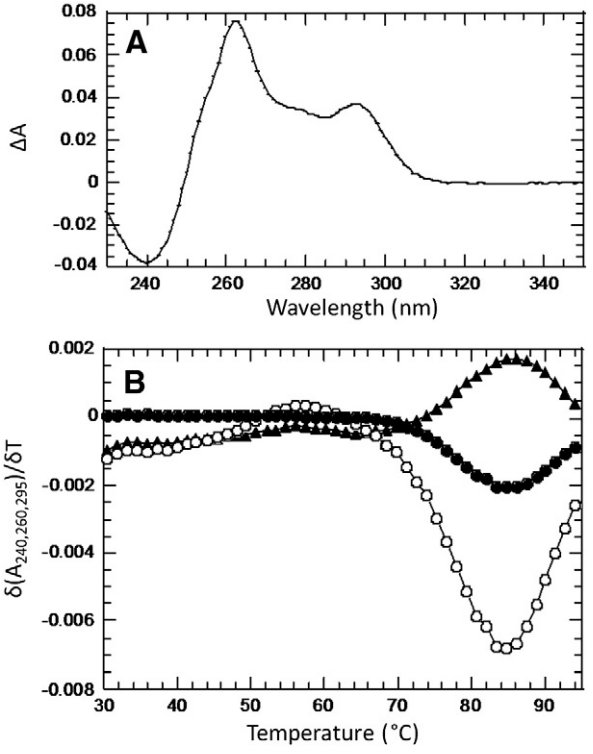

Fig. 2. (A) Absorbance difference spectra of $(GGGT)_4$ in the presence and absence of 5 mM KCl; (B) UV melting profiles of $(GGGT)_4$ at 240 nm (▲), 260 nm (○) and 295 nm (●) in the presence of 5 mM KCl.

3.3. CD and UV melting studies of $(GGGT)_4$ variants

The CD and UV melting experiments $(GGGT)_4$ suggest a parallel quadruplex topology with three G-quartets connected by chain reversal T-loops (Fig. 4B). Similar structures with single-nucleotide loops have been observed for various G-rich sequences [27,39–44]. To further distinguish between the two models shown in Fig. 4, the thermal stability and secondary structure of a series of $(GGGT)_4$ variants were investigated. The variants included deletions at the 3′-end ($(GGGT)_3GGG$, $(GGGT)_3GG$, and $(GGGT)_3G$) and single nucleotide substitutions (G2→T, G3→T, G5→T). UV unfolding experiments were performed in the presence of 1 mM KCl (Fig. 5A) or 10 mM K^+ ions (Fig. 5B) and T_m and ΔH_{vH} values determined based on these measurements are summarized in Table 1. The secondary structures of the oligonucleotides were investigated by CD measurements performed in the presence of 10 mM KCl (Fig. 6).

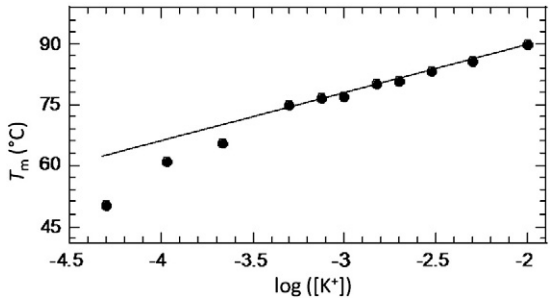

Fig. 3. The T_m dependence of $(GGGT)_4$ on the KCl concentration. The concentration of $(GGGT)_4$ is 4.5 μM.

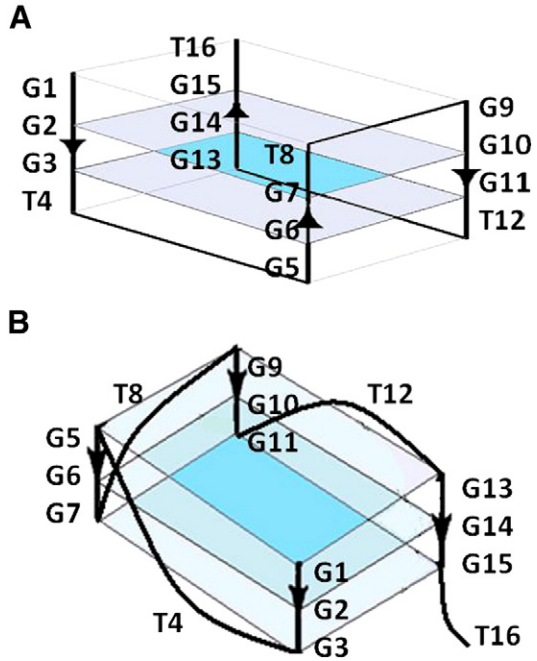

Fig. 4. Schematic diagrams showing two possible structures of $(GGGT)_4$. Anti-parallel conformation based on NMR work [9] (A), and parallel conformation suggested by us on the bases of optical and thermodynamic studies (B).

3.3.1. Deletion of T at the 3′-end

T16 is predicted to be involved in a quartet-like G-T-G-T in the antiparallel conformation and would be expected to play an important stabilizing role in this topology. In contrast, T16 is in an overhang position in the parallel structure and therefore its removal should not significantly affect the structure. As shown in Fig. 6A, deletion of this nucleotide did not have a measurable effect on the CD profile or ΔH_{vH} value (Table 1) relative to the wild-type quadruplex

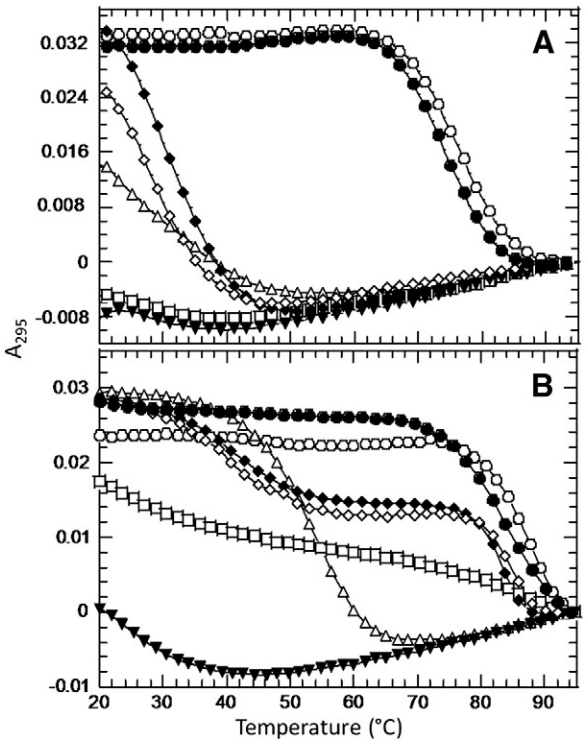

Fig. 5. UV melting profiles of $(GGGT)_4$ (●), $(GGGT)_3GGG$ (○), $(GGGT)_3GG$ (Δ), $(GGGT)_3G$ (□), G2→T (▼), G3→T (◆), and G5→T (◇) in the presence of 1 mM (A) and 10 mM (B) KCl.

Table 1
Melting temperatures and van't Hoff enthalpies derived from UV unfolding profiles in the presence 1 mM and 10 mM KCl.

Oligonucleotide	T_m (°C)		$-\Delta H_{vH}$ (kcal/mol)	
	1 mM	10 mM	1 mM	10 mM
$GGGTGGGTGGGTGGGT$ $(GGGT)_4$	74.0	90.0	62	–
$GGGTGGGTGGGTGGG$ $(GGGT)_3GGG$	75.5	92.0	63	–
$GGGTGGGTGGGTGG$ $(GGGT)_3GG$	30.0	53.0	–	46
$GGGTGGGTGGGTG$ $(GGGT)_3G$	ND	ND	ND	ND
G**T**GTGGGTGGGTGGGT G2→T	ND	ND	ND	ND
GG**T**TGGGTGGGTGGGT G3→T	30.0	40.0	–	38
GGGT**T**GGTGGGTGGGT G5→T	29.0	37.5	–	36

Melting temperatures (T_m) and van't Hoff enthalpies (ΔH_{vH}) were derived from the shapes of UV melting curves measured at a concentration of ~4 μM per strand in 10 mM Tris–HCl, pH 8.7. Values represent the average of at least three determinations and experimental errors are estimated as follows: T_m (0.5 °C) and ΔH_{vH} (±10%).

and even has a slight stabilizing effect, which is consistent with removal of a 3′ dangling nucleotide (Fig. 5). Thus, truncation of T16 clearly supports a parallel configuration of the G-tracks.

3.3.2. Deletion of GT and GGT

In contrast to the single nucleotide deletion, a two nucleotide deletion at the 3′-end has a small effect on the CD spectrum. The CD signal is reduced by ~15% at 265 nm suggesting slight unfolding of the quadruplex structure (Fig. 6B). However, UV melting experiments demonstrate strong destabilization. In the presence of 10 mM K^+ ions, the T_m is 53 °C with a sigmoidal unfolding profile characteristic to two-state transition (Fig. 5B) with the estimated enthalpy of −46 kcal/mol. Removal of three terminal nucleotides results in essentially complete unfolding of the quadruplex. The CD spectrum corresponds to that of an unstructured single-stranded DNA (Fig. 6C) and UV melting experiments do not reveal any cooperative transitions either of 1 mM or 10 mM KCl (Fig. 5).

3.3.3. G→T substitutions

Another important difference between the structures shown in Fig. 4 is the number of G-quartets; only two stacked G-quartets are present in the antiparallel orientation whereas three are present in the parallel orientation. Thus, restricting the formation of a selected G-quartet by single-nucleotide substitution should unambiguously support one of the models. For example, in the antiparallel structure, G2 and G3 are involved in the upper and lower G-quartets, respectively. Therefore, single G2→T or G3→T substitutions in either of these G-quartets should have similar effects of the quadruplex stability. In contrast, since G5 is involved in a G-T-G-T semi-quartet a G5→T substitution will likely be less destabilizing. In the case of the parallel topology, G3 and G5 are located in the upper and lower G-quartets and G→T substitutions in these positions should result in similar effects on overall stability. In contrast, G2 is involved in the middle G-quartet and substitution in this position may alter the stability to a different extent. Thus, if the antiparallel model is correct, the substitutions should follow the following pattern: G2→T = G3→T ≠ G5→T. In contrast, if the parallel model is correct, the following pattern is predicted: G3→T = G5→T ≠ G2→T. Both CD (Fig. 6E and F) and UV melting (Fig. 5) experiments indicate that the single G2→T substitution completely inhibits quadruplex formation. The effects of G3→T and G5→T mutations are almost identical. In both cases, the CD signal at 265 nm decreases by 50–60% and a new minor peak appears at 295 nm (Fig. 6E and F). As mentioned earlier, a CD signal at 295 nm is characteristic of antiparallel quadruplexes. Thus, the CD spectra indicate the simultaneous existence of two quadruplex populations, parallel and antiparallel, or alternatively, the presence of a third type of unknown structure. In agreement with CD experiments, for both modifications the UV melting experiments at 10 mM KCl reveal two separate

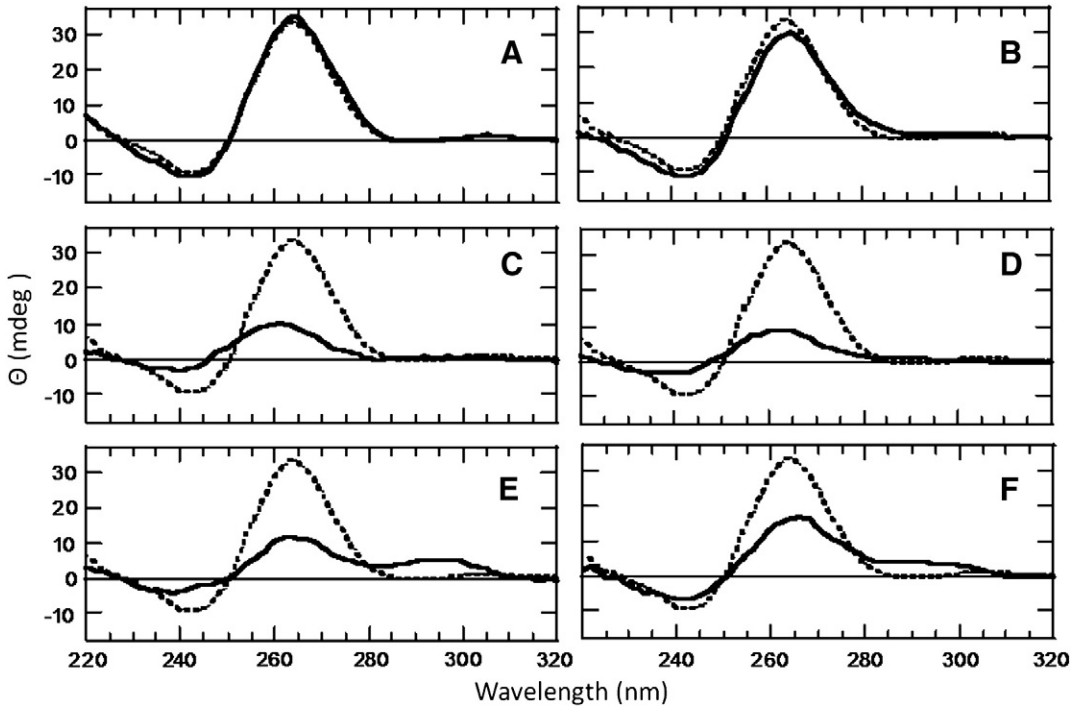

Fig. 6. CD profiles of wild-type and variant $(GGGT)_4$ in the presence of 10 mM KCl: $(GGGT)_3GGG$ (A), $(GGGT)_3GG$ (B), $(GGGT)_3G$ (C), G2→T (D), G3→T (E), and G5→T (F). Each panel contains the spectrum of $(GGGT)_4$ (dashed line) for better comparison.

transitions (Fig. 5B). Based on these data, a melting transition is observed at ~40 °C corresponding to a ΔH_{vH} value of ~40 kcal/mol. A second transition occurs at >80 °C. Taken together, the single nucleotide substitution data strongly support the formation of a parallel quadruplex by $(GGGT)_4$.

3.4. ITC experiments

ITC is a sensitive tool to measure model-independent heat of quadruplex formation upon addition of titration of K^+ ions [18,36]. For these experiments, we chose to use the most stable $(GGGT)_3GGG$ variant. To measure the complete heat of formation, the experimental temperature and salt conditions must be selected to ensure that the initial state of the oligonucleotide is completely unfolded. It is known that Cs^+ ions usually do not support quadruplex formation at room temperature. To select an appropriate experimental temperature where Cs^+-$(GGGT)_3GGG$ is completely unfolded, we performed UV melting experiments in the presence of 10 mM monovalent cations (Fig. 7). As expected, K^+-$(GGGT)_3GGG$ has a T_m ~90 °C, while Cs^+-$(GGGT)_3GGG$ demonstrates a smaller T_m of ~30 °C. Therefore, ITC experiments were performed at 50 °C where all secondary structure is disrupted. Aliquots of K^+ ions were injected into the Cs^+ salt of $(GGGT)_3GGG$ (unfolded quadruplex) solution, and the heat changes accompanying quadruplex formation and cation binding were measured. Results of a typical experiment are shown in Fig. 8. The

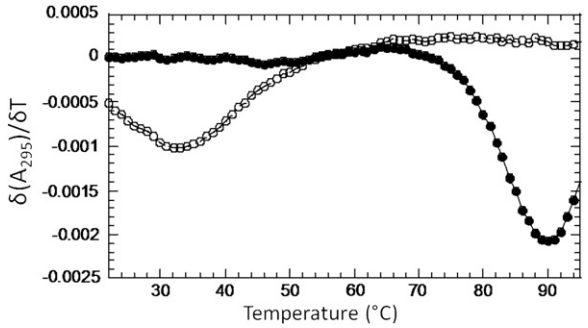

Fig. 7. UV melting profiles of $(GGGT)_3GGG$ in the presence of 10 mM CsCl (○) and 10 mM KCl (●).

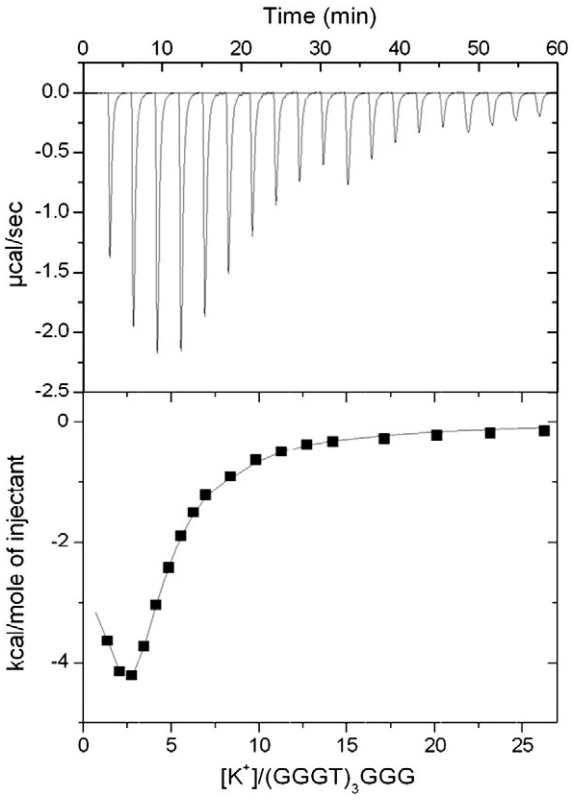

Fig. 8. A representative ITC curve of the interaction of K^+ ions $(GGGT)_3GGG$ showing exothermic heat of quadruplex formation (A). Plot showing heats of reaction as a function of molar ratio (B) corresponding to the experiment shown in the upper panel. The data are fit to a two binding-site model.

apparent discontinuity in peak size is due to an increase in volume of titrant during the experiments, which allowed us to extend the range of KCl concentration and more reliably estimate the binding parameters: number of binding sites, n, binding constants, K, and enthalpy, ΔH_{cal}. The K value corresponds to the apparent binding affinity of K^+ ions measured via the heat of quadruplex formation, since the heat of electrostatic interactions between cations and nucleic acids are negligible due to the entropic nature of the interaction [45–47].

A model with two sets of sites best fits the experimental titration curves. The solid line in Fig. 8B is a result of non-linear fitting based on this model and revealed the following parameters: $n_1 = 1.7 \pm 0.3$, $K_1 = (3.1 \pm 1.5) \times 10^6\ M^{-1}$, $\Delta H_1 = -2.8 \pm 0.4$ kcal/(mol of K^+), $n_2 = 2.8 \pm 0.2$, $K_2 = (6.6 \pm 0.5) \times 10^5\ M^{-1}$, $\Delta H_2 = -8.0 \pm 0.4$ kcal/(mol of K^+). We propose that the first binding event reflects uptake of 2 equivalents of K^+ by the inner core of the quadruplex, which is followed by binding of K^+ to T4, T8 and T12 loops (Fig. 4B). The data are consistent with earlier UV absorbance studies [9,35], which led to a proposed two-step folding model of $(GGGT)_4$.

To obtain heat per mol of the quadruplex, reverse titrations were also performed wherein Cs^+-$(GGGT)_3GGG$ was titrated into 3 mM KCl. We obtained ΔH_{cal} of −28 kcal/mol, which is around 2-fold lower than the model-dependent $\Delta H_{vH} = -62$ kcal/mol (Table 1). The discrepancy cannot be explained by electrostatic interaction (K^+ binding to the oligonucleotide in ITC experiments) since its enthalpy is negligible [45–47]. Since ΔH_{vH} is a molar enthalpy per cooperative unit, while ΔH_{cal} is the enthalpy per mol of oligonucleotide, formation of quadruplex dimers may explain the discrepancy. However, dimer formation is not consistent with our melting experiments, which indicate a two-state unfolding transition. At 50 °C the quadruplex structure formed by Cs^+ ion is unfolded (Fig. 7), however, it still possesses significant intramolecular stacking interactions. Thus, it is likely that ΔH_{cal} reflects the net effect of two opposite contributions: the endothermic heat of disruption of base-stacking in Cs^+-$(GGGT)_3GGG$ and the exothermic heat of quadruplex formation. Similar discrepancies between enthalpy values obtained from isothermal and melting experiments were observed earlier and attributed to significant base-stacking interactions within the single-stranded oligonucleotides [48,49].

4. Conclusion

Our systematic thermodynamic study of $d(GGGT)_4$ and variants with single-nucleotide modifications or 3′-end nucleotide deletions are consistent with a parallel quadruplex topology. CD studies carried out over a wide concentration range (6 μM–2 mM per strand) showed that the quadruplex maintains a single-stranded parallel fold. In the presence of 10 mM KCl, the $d(GGGT)_4$ quadruplex has a T_m of 90 °C and removal of the terminal 3′-T further stabilizes the structure. Systematic thermodynamic analyses of $d(GGGT)_4$ and variants containing sequence modifications or missing specific nucleotides are consistent with a parallel quadruplex fold. An ITC study of K^+ interaction with $(GGGT)_3GGG$ suggests a two-step binding model. We propose that the first step involves two equivalents of K^+ between the G-quartets followed by binding three K^+ ions to the T-loops.

References

[1] M.J. McEachern, A. Krauskopf, E.H. Blackburn, Telomeres and their control, Annu. Rev. Genet. 34 (2000) 331–358.
[2] C. Schaffitzel, I. Berger, J. Postberg, J. Hanes, H.J. Lipps, A. Pluckthun, In vitro generated antibodies specific for telomeric guanine-quadruplex DNA react with Stylonychia lemnae macronuclei, Proc. Natl Acad. Sci. U.S.A. 98 (2001) 8572–8577.
[3] R.D. Gray, L. Petraccone, J.O. Trent, J.B. Chaires, Characterization of a K^+-induced conformational switch in a human telomeric DNA oligonucleotide using 2-aminopurine fluorescence, Biochemistry 49 (2010) 179–194.
[4] N. Maizels, Dynamic roles for G4 DNA in the biology of eukaryotic cells, Nat. Struct. Mol. Biol. 13 (2006) 1055–1059.
[5] S. Burge, G.N. Parkinson, P. Hazel, A.K. Todd, S. Neidle, Quadruplex DNA: sequence, topology and structure, Nucleic Acids Res. 34 (2006) 5402–5415.
[6] A. De Cian, G. Cristofari, P. Reichenbach, E. De Lemos, D. Monchaud, M.P. Teulade-Fichou, K. Shin-Ya, L. Lacroix, J. Lingner, J.L. Mergny, Reevaluation of telomerase inhibition by quadruplex ligands and their mechanisms of action, Proc. Natl Acad. Sci. U.S.A. 104 (2007) 17347–17352.
[7] H.M. So, K. Won, Y.H. Kim, B.K. Kim, B.H. Ryu, P.S. Na, H. Kim, J.O. Lee, Single-walled carbon nanotube biosensors using aptamers as molecular recognition elements, J. Am. Chem. Soc. 127 (2005) 11906–11907.
[8] L.C. Bock, L.C. Griffin, J.A. Latham, E.H. Vermaas, J.J. Toole, Selection of single-stranded DNA molecules that bind and inhibit human thrombin, Nature 355 (1992) 564–566.
[9] N. Jing, M.E. Hogan, Structure-activity of tetrad-forming oligonucleotides as a potent anti-HIV therapeutic drug, J. Biol. Chem. 273 (1998) 34992–34999.
[10] N. Jing, C. Marchand, J. Liu, R. Mitra, M.E. Hogan, Y. Pommier, Mechanism of inhibition of HIV-1 integrase by G-tetrad-forming oligonucleotides in Vitro, J. Biol. Chem. 275 (2000) 21460–21467.
[11] R.F. Rando, J. Ojwang, A. Elbaggari, G.R. Reyes, R. Tinder, M.S. McGrath, M.E. Hogan, Suppression of human immunodeficiency virus type 1 activity in vitro by oligonucleotides which form intramolecular tetrads, J. Biol. Chem. 270 (1995) 1754–1760.
[12] B.I. Kankia, Optical absorption assay for strand-exchange reactions in unlabeled nucleic acids, Nucleic Acids Res. 32 (2004) e154.
[13] J.L. Mergny, A.T. Phan, L. Lacroix, Following G-quartet formation by UV-spectroscopy, FEBS Lett. 435 (1998) 74–78.
[14] P.A. Rachwal, K.R. Fox, Quadruplex melting. Meth. 43 (2007) 291–301.
[15] B.I. Kankia, A real-time assay for monitoring nucleic acid cleavage by quadruplex formation, Nucleic Acids Res. 34 (2006) e141.
[16] B.I. Kankia, Self-dissociative primers for nucleic acid amplification and detection based on DNA quadruplexes with intrinsic fluorescence, Anal. Biochem. 409 (2011) 59–65.
[17] N. Jing, R.F. Rando, Y. Pommier, M.E. Hogan, Ion selective folding of loop domains in a potent anti-HIV oligonucleotide, Biochemistry 36 (1997) 12498–12505.
[18] B.I. Kankia, G. Barany, K. Musier-Forsyth, Unfolding of DNA quadruplexes induced by HIV-1 nucleocapsid protein, Nucleic Acids Res. 33 (2005) 4395–4403.
[19] P.A. Rachwal, T. Brown, K.R. Fox, Sequence effects of single base loops in intramolecular quadruplex DNA, FEBS Lett. 581 (2007) 1657–1660.
[20] B.I. Kankia, L.A. Marky, DNA, RNA, and DNA/RNA oligomer duplexes: a comparative study of their stability, heat, hydration and $Mg(2+)$ binding properties, J. Phys. Chem. B 103 (1999) 8759–8767.
[21] L.A. Marky, K.J. Breslauer, Calculating thermodynamic data for transitions of any molecularity from equilibrium melting curves, Biopolymers 26 (1987) 1601–1620.
[22] A. Matsugami, K. Ouhashi, M. Kanagawa, H. Liu, S. Kanagawa, S. Uesugi, M. Katahira, An intramolecular quadruplex of (GGA)(4) triplet repeat DNA with a G:G:G:G tetrad and a G(:A):G(:A):G(:A):G heptad, and its dimeric interaction, J. Mol. Biol. 313 (2001) 255–269.
[23] C.F. Tang, R.H. Shafer, Engineering the quadruplex fold: nucleoside conformation determines both folding topology and molecularity in guanine quadruplexes, J. Am. Chem. Soc. 128 (2006) 5966–5973.
[24] S. Paramasivan, I. Rujan, P.H. Bolton, Circular dichroism of quadruplex DNAs: applications to structure, cation effects and ligand binding, Methods 43 (2007) 324–331.
[25] C.C. Hardin, M.J. Corregan, D.V. Lieberman, B.A. Brown 2nd, Allosteric interactions between DNA strands and monovalent cations in DNA quadruplex assembly: thermodynamic evidence for three linked association pathways, Biochemistry 36 (1997) 15428–15450.
[26] M. Lu, Q. Guo, N.R. Kallenbach, Thermodynamics of G-tetraplex formation by telomeric DNAs, Biochemistry 32 (1993) 598–601.
[27] A.T. Phan, V. Kuryavyi, J.B. Ma, A. Faure, M.L. Andreola, D.J. Patel, An interlocked dimeric parallel-stranded DNA quadruplex: a potent inhibitor of HIV-1 integrase, Proc. Natl Acad. Sci. U.S.A. 102 (2005) 634–639.
[28] N. Smargiasso, F. Rosu, W. Hsia, P. Colson, E.S. Baker, M.T. Bowers, E. De Pauw, V. Gabelica, G-quadruplex DNA assemblies: loop length, cation identity, and multimer formation, J. Am. Chem. Soc. 130 (2008) 10208–10216.
[29] A.T. Phan, D.J. Patel, Two-repeat human telomeric d(TAGGGTTAGGGT) sequence forms interconverting parallel and antiparallel G-quadruplexes in solution: distinct topologies, thermodynamic properties, and folding/unfolding kinetics, J. Am. Chem. Soc. 125 (2003) 15021–15027.
[30] I.N. Rujan, J.C. Meleney, P.H. Bolton, Vertebrate telomere repeat DNAs favor external loop propeller quadruplex structures in the presence of high concentrations of potassium, Nucleic Acids Res. 33 (2005) 2022–2031.
[31] S. Masiero, R. Trotta, S. Pieraccini, S. De Tito, R. Perone, A. Randazzo, and G.P. Spada, A non-empirical chromophoric interpretation of CD spectra of DNA G-quadruplex structures. Org Biomol Chem 8 2683–92.
[32] R.F. Macaya, P. Schultze, F.W. Smith, J.A. Roe, J. Feigon, Thrombin-binding DNA aptamer forms a unimolecular quadruplex structure in solution, Proc. Natl Acad. Sci. U.S.A. 90 (1993) 3745–3749.
[33] K.Y. Wang, S. McCurdy, R.G. Shea, S. Swaminathan, P.H. Bolton, A DNA aptamer which binds to and inhibits thrombin exhibits a new structural motif for DNA, Biochemistry 32 (1993) 1899–1904.
[34] K. Padmanabhan, K.P. Padmanabhan, J.D. Ferrara, J.E. Sadler, A. Tulinsky, The structure of alpha-thrombin inhibited by a 15-mer single-stranded DNA aptamer, J. Biol. Chem. 268 (1993) 17651–17654.
[35] N. Jing, C. Marchand, Y. Guan, J. Liu, L. Pallansch, C. Lackman-Smith, E. De Clercq, Y. Pommier, Structure-activity of inhibition of HIV-1 integrase and virus replication by G-quartet oligonucleotides, DNA Cell Biol. 20 (2001) 499–508.

[36] B.I. Kankia, L.A. Marky, Folding of the thrombin aptamer into a G-quadruplex with Sr(2+): stability, heat, and hydration, J. Am. Chem. Soc. 123 (2001) 10799–10804.
[37] B.I. Kankia, Mg^{2+}-induced triplex formation of an equimolar mixture of poly(rA) and poly(rU), Nucleic Acids Res. 31 (2003) 5101–5107.
[38] P. Wallimann, R.J. Kennedy, J.S. Miller, W. Shalongo, D.S. Kemp, Dual wavelength parametric test of two-state models for circular dichroism spectra of helical polypeptides: anomalous dichroic properties of alanine-rich peptides, J. Am. Chem. Soc. 125 (2003) 1203–1220.
[39] A.T. Phan, Y.S. Modi, D.J. Patel, Propeller-type parallel-stranded G-quadruplexes in the human c-myc promoter, J. Am. Chem. Soc. 126 (2004) 8710–8716.
[40] A. Ambrus, D. Chen, J. Dai, R.A. Jones, D. Yang, Solution structure of the biologically relevant G-quadruplex element in the human c-MYC promoter Implications for G-quadruplex stabilization, Biochemistry 44 (2005) 2048–2058.
[41] J. Dai, T.S. Dexheimer, D. Chen, M. Carver, A. Ambrus, R.A. Jones, D. Yang, An intramolecular G-quadruplex structure with mixed parallel/antiparallel G-strands formed in the human BCL-2 promoter region in solution, J. Am. Chem. Soc. 128 (2006) 1096–1098.
[42] A.T. Phan, V. Kuryavyi, S. Burge, S. Neidle, D.J. Patel, Structure of an unprecedented G-quadruplex scaffold in the human c-kit promoter, J. Am. Chem. Soc. 129 (2007) 4386–4392.
[43] A.K. Todd, S.M. Haider, G.N. Parkinson, S. Neidle, Sequence occurrence and structural uniqueness of a G-quadruplex in the human c-kit promoter, Nucleic Acids Res. 35 (2007) 5799–5808.
[44] V. Kuryavyi, A.T. Phan, D.J. Patel, Solution structures of all parallel-stranded monomeric and dimeric G-quadruplex scaffolds of the human c-kit2 promoter, Nucleic Acids Res. 38 (2010) 6757–6773.
[45] H. Krakauer, A thermodynamic analysis of the influence of simple mono-and divalent cations on the conformational transitions of polynucleotide complexes, Biochemistry 13 (1974) 2579–2589.
[46] T. Ohyama, J.A. Cowan, An approach to the evaluation of RNA solution structure and metal coordination chemistry by titration calorimetry, J. Biol. Inorg. Chem. 2 (1997) 553–554.
[47] P.D. Ross, J.T. Shapiro, Heat of interaction of DNA with polylysine, spermine, and Mg^{++}, Biopolymers 13 (1974) 415–416.
[48] I. Jelesarov, C. Crane-Robinson, P.L. Privalov, The energetics of HMG box interactions with DNA: thermodynamic description of the target DNA duplexes, J. Mol. Biol. 294 (1999) 981–995.
[49] G. Vesnaver, K.J. Breslauer, The contribution of DNA single-stranded order to the thermodynamics of duplex formation, Proc. Natl Acad. Sci. U.S.A. 88 (1991) 3569–3573.